VOL. 3, NO. 3, JUNE 2008 ISSN 1819-6608
ARPN Journal of Engineering and Applied Sciences


www.arpnjournals.com

FINITE ELEMENT ANALYSIS OF TUNNELS USING THE ELASTOPLASTIC-VISCOPLASTIC BOUNDING SURFACE MODEL

Qassun S. Mohammed Shafiqu, Mohd R. Taha and Zamri H. Chik
Department of Civil and Structural Engineering, University Kebangsaan Malaysia, Malaysia
E-mail: qassun@yahoo.com

ABSTRACT

Finite element analyses of tunnels in saturated porous medium were performed using the elastoplastic-viscoplastic bounding surface model. In this paper, the model and the finite element formulation are described and examples of model prediction and accuracy of the finite element formulation are given. The transient analysis of tunnel problem is then carried out, and the comparison of the finite element results with the field measurements demonstrate the ability of the bounding surface model to solve problems of tunneling in saturated porous medium.

Keywords: finite element analysis, model, bounding surface, consolidation, tunnels, viscoplasticity.

INTRODUCTION

Excavation of a tunnel causes stress changes, which in turn produce deformations that occur during and long after the tunnel's excavation. When a tunnel is excavated in saturated ground, the following two-types of time-dependent behavior occur in the surrounding ground. The first is due to the intrinsic rate-dependent characteristics of the materials, such as creep deformation. The second is caused by the movement of pore water due to the change of pore water pressure distributing in the surrounding ground.

The finite element method has been employed in the past to perform time-dependent behavior of tunnel. For example, Zienkiewicz *et al.* (1974) studied the problem of rock relaxation around a lined tunnel using elasto-viscoplastic Mohr-Coulomb FEM. Kamemura and Kimura (1981) studied the time-dependent plastic behavior around tunnel basing on the constitutive equations derived from the elasto-viscoplastic material behavior theory. Finno and Clough (1985) conducted 2-D analyses of a 3.7m diameter EPB shield tunnel for the San Francisco Clean Water Project in the transverse and longitudinal directions using the modified Cam-clay soil model and compared the results with site data. While Pan and Hudson (1988) used the Mohr-Coulomb, Druker-Prager and Hoek-Brown yield criteria to study the behavior of a circular tunnels driven in homogeneous, isotropic, elasto-viscoplastic medium. Adachi *et al.* (1995) carried out a FEM coupling analysis for the change of mechanical behavior of the tunnel surrounding ground using the Biot's consolidation theory and "Adachi-Oka's" elastoplastic constitutive law with strain-hardening and strain-softening. Recently, Sowboda and Abu-Krisha (1999) used the FEM to analyze three-dimensional coupled linear flow for Tunnel Boring Machine (TBM) used in saturated porous medium. An isoparametric quadratic solid consolidation elastic soil model is used for this analysis. Results of this study indicate that a realistic modelling of soil behaviour, especially the distribution shape of the excess pore water pressure around the TBM tunnels during the construction stages and its dissipation during the consolidation time can be assessed. Xiaoli *et al.* (2002) evaluate the effects of intermediate principal stress on the displacement around tunnels using a unified yield criterion and a non-associated flow rule. The time-dependent behavior is simulated by Kelvin model, consisting of a spring and a cohesive element with parallel connection. The effects of dilatancy and creep of rock are considered in the solution. Kasper and Meschke (2004) presented the simulation of a tunnel advance in soft cohesive soil below the ground water table using a three-dimensional finite element simulation model for shield-driven tunnel excavation. A Cam-Clay plasticity model is used to describe the material behaviour of cohesive soils. Shalabi (2005) investigated ground movement and contact pressure on the lining of Stillwater Tunnel (Utah, USA) using axisymmetirc finite element analysis. Power law and hyperbolic creep models were used to model ground squeezing and to show the differences in the results between the two models. The effectiveness of a time-dependent swelling model that considers the three-dimensional stress effect is presented by Hawlader *et al.* (2006). And a finite element algorithm incorporating this constitutive model is used for a numerical analysis of tunnels in shales or shaly rocks endure time-dependent swelling effects.

In the following sections, the proposed model and the finite element formulation are described and examples of model prediction and accuracy of the finite element formulation are given. An elastoplastic-viscoplastic analysis of advanced shield tunneling in soils is then studied using the model and comparison the results with site data is carried out.

THE ELASTOPLASTIC-VISCOPLASTIC BOUNDING SURFACE MODEL

Details of the elastoplastic-viscoplastic formulation, the numerical implementation of the model and the parameters associated with the model are available in Kaliakin and Dafalias (1990). Therefore, only the elastoplastic-viscoplastic rate relations are given here.

The total strain rate is consisting of three parts: elastic, plastic and viscoplastic strain.

$$\dot{\varepsilon}_{ij} = \dot{\varepsilon}^{e}_{ij} + \dot{\varepsilon}^{p}_{ij} + \dot{\varepsilon}^{v}_{ij} \quad (1)$$

The inverse form of the constitutive relations is obtained as:

$$\dot{\sigma}_{ij} = D_{ijkl}\dot{\varepsilon}_{kl} - V_{ij} \quad (2)$$

$$D_{ijkl} = \left[2G\,\delta_{ik}\delta_{jl} + \left(K - \frac{2}{3}G \right)\delta_{ij}\delta_{kl} \right]_{ij} \quad (3)$$

$$-\left\{ 3K\,F_{,\bar{I}}\delta_{kl} + \frac{G}{J}F_{,\bar{J}}s_{kl} + \frac{\sqrt{3}}{bJ}\frac{G\,F_{,\alpha}}{\cos 3\alpha}\left[\frac{1}{J^2}\left(s_{kn}s_{nl} - \frac{3}{2}\frac{S^3}{J^2}s_{kl} \right) - \frac{2}{3}\delta_{kl} \right] \right\}$$

$$\left\{ 3K\,F_{,\bar{I}}\delta_{ij} + \frac{G}{J}F_{,\bar{J}}s_{ij} + \frac{\sqrt{3}}{bJ}\frac{G\,F_{,\alpha}}{\cos 3\alpha}\left[\frac{1}{J^2}\left(s_{in}s_{nj} - \frac{3}{2}\frac{S^3}{J^2}s_{ij} \right) - \frac{2}{3}\delta_{ij} \right] \right\} \frac{\Lambda}{D}$$

The viscoplastic contribution is given by:

$$V_{ij} = \langle \phi \rangle \left\{ 3K\,F_{,\bar{I}}\delta_{ij} + \frac{G}{J}F_{,\bar{J}}s_{ij} + \frac{\sqrt{3}}{bJ}\frac{G\,F_{,\alpha}}{\cos 3\alpha} \right. \quad (4)$$

$$\left[\frac{1}{J^2}\left(s_{ij}s_{nj} - \frac{3}{2}\frac{S^3}{J^2}s_{ij} \right) - \frac{2}{3}\delta_{ij} \right]$$

$$\left\{ 1 - \left\{ 9K\left(F_{,\bar{I}} \right)^2 + G\left(F_{,\bar{J}} \right)^2 + G\left(\frac{F_{,\alpha}}{bJ} \right)^2 \right.\right.$$

$$\left.\left. + \bar{K}_p \left[\frac{1}{b} - C\left(1 - \frac{1}{b} \right)\frac{F_{,\bar{I}}}{F_{,I_o}} \right] \right\} \frac{\Lambda}{D} \right\}$$

In the above expressions

$$\Lambda = \begin{cases} 1 & \text{if } L > 0 \\ 0 & \text{if } L \le 0 \end{cases} \quad (5)$$

$$D = K_p + 9K\left(F_{,\bar{I}} \right)^2 + G\left(F_{,\bar{J}} \right)^2 + G\left(\frac{F_{,\alpha}}{bJ} \right)^2 \quad (6)$$

where K and G represent the elastic bulk and shear moduli, respectively, δ_{ij} is the Kronecker delta, K_p the plastic modulus, I and J are the stress invariants, $1 \le b \le \infty$ and F represents the analytical expression of the bounding surface.

Required model parameters

The material parameters used to operate the elastoplastic-viscoplastic bounding surface model are (Kaliakin, 2005):

λ = Slope of consolidation line,

κ = Slope of swelling line,

$N(\alpha)$ = Slope of critical state line, $N_c = N$ in compression, $N_e = N$ in extension,

$R(\alpha)$ = $R > 1$ defines the point $I_1 = I_o / R$ (Figure, 1), which together with point J_1 define the coordinates of point H which is the intersection of $F = 0$ and CSL, $R_c = R$ in compression, $R_e = R$ in extension,

C = Parameter which determines the center of the bounding surface $I_c = CI_o$. And its value ranges between $0 \le C < 1$.

s = Parameter which determines indirectly "elastic nucleus". For $s = 1$ the elastic nucleus degenerates to point I_c center of bounding surface and as $s \to \infty$ the elastic nucleus expand towards the bounding surface.

h = Slope-hardening factor, which is a function of lode angle (α), $h_c =$ for compression $\left(h_c = h(\pi/6)\right)$, $h_e =$ for extension $\left(h_e = h(-\pi/6)\right)$

a and w = Hardening parameters

s_v = Viscoplastic zone parameter $s_v\,(1 < s_v \le \infty)$

V= Viscoplastic parameter in which small values of V the viscous response occurs very rapidly and if V is large the viscoplastic strain is greatly reduced, resulting in little change in the overall response with time

n = Viscoplastic parameter which increase it have similar effect on the response as do increase in V, through variations in the latter have a greater influence on the initial slope of the response curve

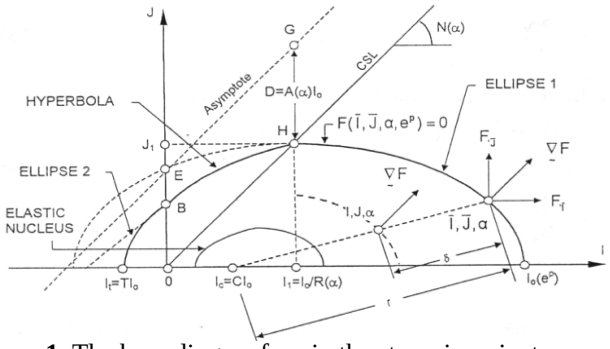

Figure-1. The bounding surface in the stress invariants pace (Dafalias and Herrmann, 1986).

FINITE ELEMENT FORMULATION

The elastoplastic-viscoplastic bounding surface model described above is incorporated in a finite element program, which has the feature of modeling two-dimensional (plane strain and axisymmetric) geotechnical problems such as consolidation, multistage excavation, written by FORTRAN90 language. In addition to the elastoplastic-viscplastic model, the program allows one to assign linear elastic behavior to any part of the problem geometry. Description of all of the program features is beyond the scope of this paper, and a brief summary of the features relevant to this study is given below:

Excavation algorithm

The aim of the analysis is that when a portion of material is excavated, either in open excavations or an

enclosed tunnel, forces must be applied along the excavated surface such that: (1) The new "free surface" is stress free, and (2) The bounding forces at the i^{th} stage of an excavation are given as (Brown and Booker, 1985):

$$F_i = \int_{Vi} B^T \sigma_{i-1} dV - \int_{Vi} N^T \gamma \, dV \quad (7)$$

where B is the strain-displacement matrix, N the element shape functions. The first term is the nodal internal resisting force vector due to the stresses in the removed elements, and the second term the reversal of the nodal body-load forces (of the removed elements) assuming that γ (the body-load due to gravity) is acting downwards. Also the total stress in Equation (7) was obtained by adding the effective stress computed at the Gauss points from the solid phase of the analysis (8-node), to the pore pressures interpolated from their nodal values of the fluid phase (4-node).

Transient formulation

In the case of an excavation, the loading is time-dependent, so an incremental formulation was used in the following work producing the matrix version of the Biot equation at the element level presented below (Lewis and Schrefler, 1987).

$$\begin{bmatrix} K & L \\ L^T & S+\overline{\alpha}H\Delta t_k \end{bmatrix} \begin{Bmatrix} \overline{u} \\ \overline{p} \end{Bmatrix} = \begin{bmatrix} K & L \\ L^T & S-(1-\overline{\alpha})H\Delta t_k \end{bmatrix} \begin{Bmatrix} \overline{u} \\ \overline{p} \end{Bmatrix} + \begin{Bmatrix} dF/dt + C \\ \overline{F} \end{Bmatrix} \quad (8)$$

where K = element solid stiffness matrix, L = element coupling matrix, H = element fluid stiffness matrix, $\overline{u}$ = change in nodal displacements, $\overline{p}$ = change in nodal excess pore-pressures, S = the compressibility matrix, $\overline{F}$ = load vector, Δt = calculation time step, $\overline{\alpha}$ = time stepping parameter (=1 in this work), dF/dt = change in nodal forces.

VERIFICATION PROBLEMS

Transient analysis of excavation in elastic soils

The analysis was performed on the single column of elements (Figure-2). The soil was assumed to be elastic and initially stress free and have the drained properties shown in Figure-2.

Removing the top element and allowing the column to drain show the distribution of non-dimensional excess pore pressures throughout the column in Figure (3a) for different values of the time factor. The obtained results are well compared with Terzaghi's (1943) one-dimensional theory and with the numerical results by Holt and Griffiths (1992). Figure (3b) shows a significant heave at node 17 (Figure-2) due to the described excavation procedures this time with the excavated region being removed in one, two and three stages, giving again good agreement with the theoretical and numerical solutions.

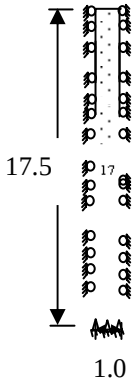

Soil parameters for the elastic soil
after Holt and Griffiths, (1992).
Young's modulus, E (kPa)= 1.0
Poisson's ratio, ν =0.0
Coefficient of lateral stress at rest, K_o =1.0
Permeability in the x-direction, k_x (m/sec)= 10
Permeability in the y-direction, k_y (m/sec)= 10
Saturated unit weight of the soil, γ_s (kN/m^3)= 20

Elements removed during excavation

Notes:
- All dimensions are in meters
- All elements equal unit thickness and of equal heights

Figure-2. Finite element mesh for the one-dimensional excavation problem.

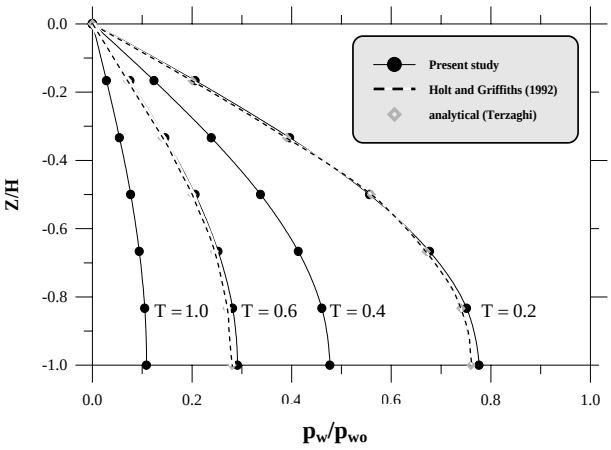

Figure-3a. Excess pore pressure

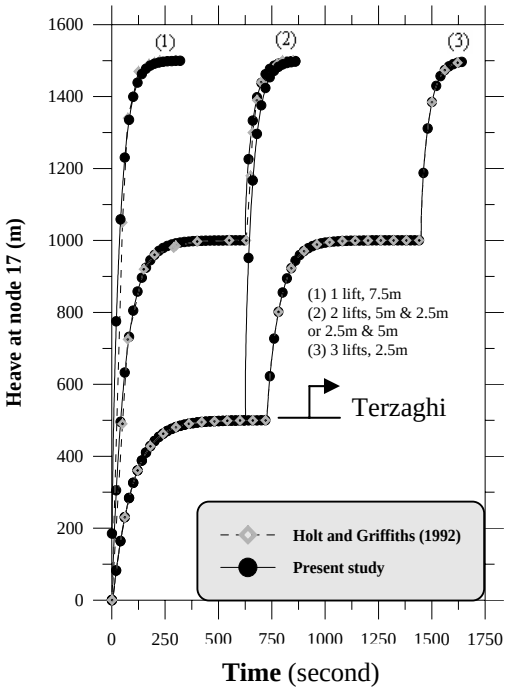

Figure-3b. Heave at node 17 with time.

Simulation of drained triaxial creep response for normally consolidated clay

This problem is reported experimentally by Lacerda (1976), which made compression tests on fine-grained, normally consolidated organic silty clay known as San Francisco Bay Mud. The specimens taken from isotropically normally consolidated to different confining pressures and then sheared at a quite low rate of loading, thus viscoplastic effects have a chance to become active. This response, against which the model simulations are compared, is depicted by discrete symbols in Figure (4). The parameters used for the model are listed in Table-1 as reported by Kaliakin and Dafalias (1990).

The results support the verification process of the used program, and indicate that the model successfully represents the viscoplasticity behavior of the material.

Table-1. Bounding surface parameters (after Kaliakin and Dafalias, 1990).

parameter	Value	parameter	Value
λ	0.37	s_p	1.0
κ	0.054	h	1.0
υ	[a]	a	1.2
M_c	1.40	w	5.0
M_e	0.95	s_v	3.20
R	2.10	V (kPa – min)	9.8×10^7
C	0.0	n	4.0

[a] Instead of the Poisson's ratio υ, the Shear modulus G is given equal to 23540kPa.

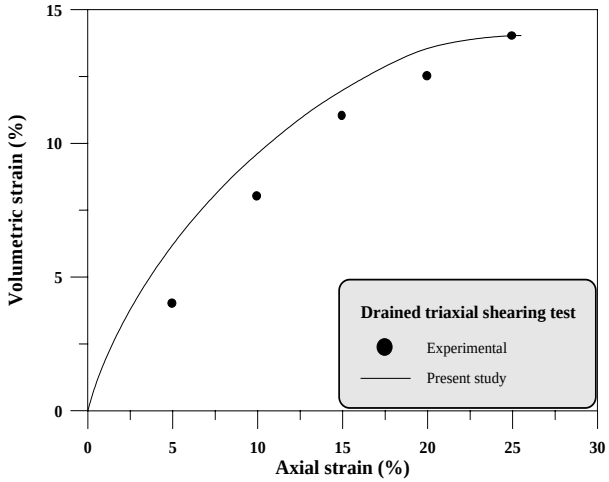

Figure-4a. Volumetric strain-axial strain curve for drained triaxial creep response of normally consolidated clay.

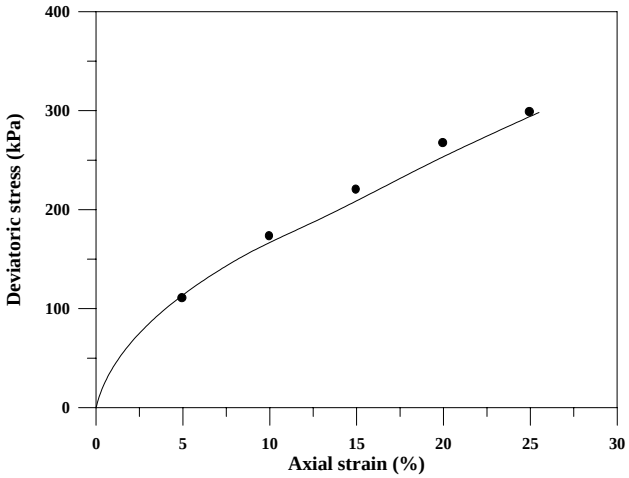

Figure-4b. shear stress-strain curve for drained triaxial creep response of normally consolidated clay.

ELASTOPLASTIC-VISCOPLASTIC ANALYSES OF ADVANCED SHIELD TUNNELING IN SOILS

Soft ground tunneling is often challenging because of the occurrence of soft water-bearing soils and environmental constraints that require strict ground movement control. Tunneling in such conditions has been made possible due to significant technological advances that were achieved over the past twenty to thirty years. These include the development of shield tunneling.

In the first application of the shield technology in the U.S.A, a 3.7m diameter EPB shield was used in 1981 to derive a 915m long tunnel for the San Francisco Clean Water Project (Clough *et. al.*, 1983). The tunnel known as the N-2 contract is located on the northeastern portion of the San Francisco Peninsula several blocks from the waterfront and San Francisco Bay.

Finno and Clough (1985) conducted 2-D analyses in plane strain in the transverse and longitudinal directions, and compared the results with site data in the N-2 contract project. Modified Cam-clay model for soil was used.

Simulation of the tunneling process in the transverse section case involved four action stages beyond the gravity stress environment (Figure-5):

1. Incrementally application of outward elliptically distributed radial pressures to the tunnel periphery (heaving stage induced by passage of tunnel shield).
2. The effects of tail void closure are accounted for by incrementally applying a uniform unloading pressure around the tunnel periphery. The node at the tunnel crown monitors inward soil movements; when this node has moved an amount equal to the theoretical size of the tail void, the void is considered closed, and the lining is installed. Note that the soil is not assumed to recover its initial heave prior to tail void closure. By avoiding this assumption, the actual three-dimensional conditions around the shield are simulated. In the field, as the shield advances and heaves the soil located initially at the shield periphery, soil from the face area will be squeezed outward and maintain contact with the shield. No actual gap exists between the shield and the soil as a result of the heaving process. Thus, the only gap which can close after heaving is that created by tail void.
3. Activate the tunnel lining after the gap has been closed. This is accomplished by first changing the material parameters of the elements inside the tunnel periphery from very low stiffness to stiffnesses representative of the actual lining. Then the remainder of the excavation forces is incrementally applied. The remainder of the excavation forces is computed by calculating equivalent nodal forces from the unrelieved stresses in the soil elements around the tunnel.
4. Remaining excess pore pressure dissipates in this stage.

In this section, the adequacy of the finite element solution can be checked against the field data observed and numerical results predicted. The finite element mesh for the transverse section analyses and the subsurface conditions are shown in Figure-6. The rubble fill and Colluvial layers were simulated using the elastic model. The parameters are given in Table-2. While, the Recent Bay Mud was modeled using the elastoplastic-viscoplastic bounding surface model and the parameters are given in Table-3. The lining system consisted of bolted steel segments with a thickness of 6mm which were erected in the tail of the shield. The outside diameter of the erected ring was 3.55m. The parameters of the lining are given in Table-4.

Movements of the ground surface directly above the centerline of the tunnel are shown in Figure-7 as a function of time. Also, Measured and predicted values of surface settlements for a transverse section at a period of 150 days following tunneling are used to define the settlement bowl above the tunnel in Figure-8. The following conclusions can be drawn:

- The elastic soil model significantly overestimates the initial heave and does not exhibit consolidation effects.
- Both the elastoplastic-viscoplastic bounding surface and the modified Cam-clay models yielded reasonable behavior trends when the best construction simulation procedure was used. However, the bounding surface model seemed to predict details of the response better than the Cam-clay model when compared with the field data available.

Table -2. Soil parameters for elastic model (after Finno and Clough,1985).

Soil parameters	**Random fill**	**Colluvium**
Poisson's ratio, ν	0.3	0.35
Failure ratio, R_f	0.49	0.49
Effective friction angle, ϕ_f	30^o	20^o
Cohesion, c (kN/m^3)	47	157
Modulus constant, K	400	945
Total unit weight, γ_t (kN/m^3)	15.7	19.63

Table-3. Bounding surface parameters for San Francisco Bay Mud (after Kaliakin and Dafalias, 1991).

Parameter	**Value**	**Parameter**	**Value**
λ	0.326	h_e	10.0
κ	0.043	a	1.2
G	23540 kPa	w	5.0
M_c	1.2	s_v	3.2
M_e	1.2	V	9.8×10^7 kPa – min
R	2.1	n	4.0
C	0.0	m	0.02
s_p	1.0	$k_x = k_y$	8.5344×10^{-4} m/day
h_c	10.0	e_{in}	3.27

Table-4. Parameters for the tunnel steel lining (after Finno and Clough,1985).

Steel lining parameters	**value**
Young's modulus, E_s (MPa)	200000
Poisson's ratio, ν_s	0.3

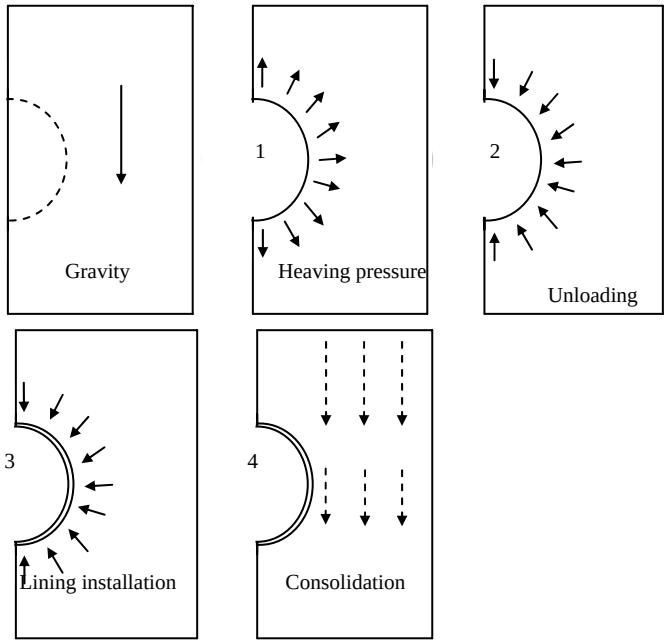

Figure-5. Stages in simulation of shield tunneling process.

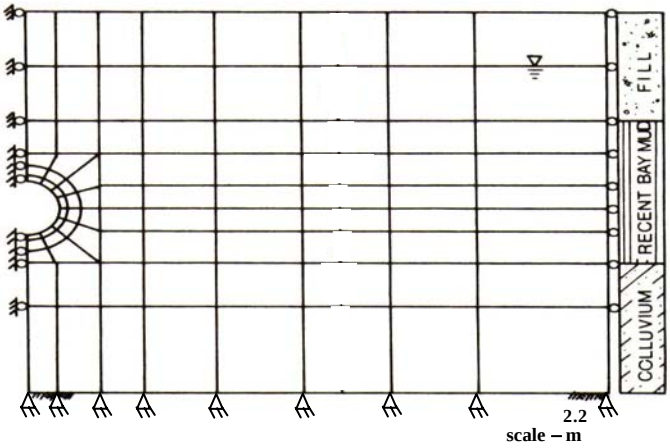

Figure-6. Finite element mesh for transverse section analysis of N-2 case.

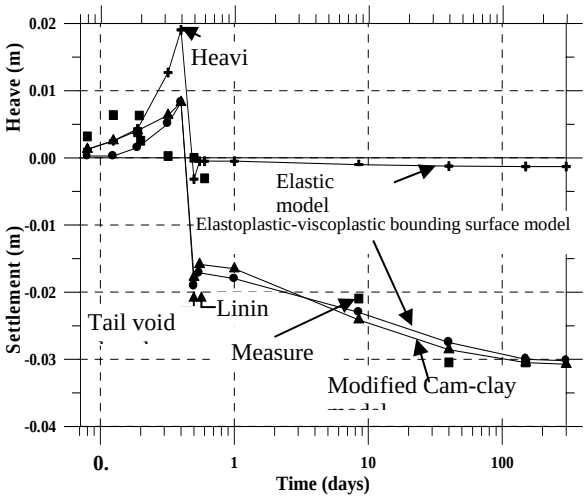

Figure-7. Predicted and observed centerline surface movements with time for shield tunneling problem.

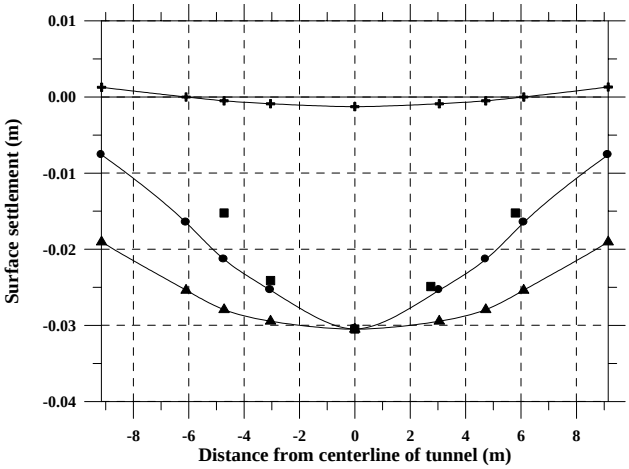

Figure-8. Predicted and observed surface settlement bowl 150 days after shield passage.

CONCLUSIONS

In this paper, a fully transient program for the analysis of tunnel problems excavated in saturated porous media is develop. This was to allow the transition between the states of drained and undrained behavior to be investigated. An algorithm for carrying out such an analysis has been presented. The transient response of the saturated porous media was based on the theory of consolidation developed by Biot (1941). Also it should be emphasized that the results presented herein were based on elastic and elastoplastic-viscoplastic bounding surface soil models, knowing that the latter allow the inelastic deformations to occur for stress points within the bounding surface.

The algorithm was validated against one-dimensional theory for both pore pressure and displacement predictions, while the elastoplastic-viscoplastic bounding surface model implementation was verified using experimental triaxial test results. Then the results of elastoplastic-viscoplastic analyses of advanced shield tunneling in soils are presented. The following conclusions were observed:

- The elastic soil model under-predicted the displacements along the tunnel wall when compared to the displacements predicted by a bounding surface model. And in the case of shield tunneling through a soft silt and clay deposit, it significantly overestimates the initial heave and does not exhibit consolidation effects
- Both the elastoplastic-viscoplastic bounding surface and the modified Cam-clay models yielded reasonable behavior trends when the best construction simulation procedure was used. However, the bounding surface model seemed to predict details of the response better than the Cam-clay model when compared with the field data available.

REFERENCES

Adachi T., Jun L., Akinori K. and Feng Z. 1995. Numerical Analysis of Biot Consolidation Problem Based on An Elasto-Plastic Constitutive Model with Strain Softening in Tunneling. Proceedings 7th Geotechnical Symposium, Nagoya, Japan. pp. 105-110.

Biot M. A. 1941. General Theory of Three-Dimensional Consolidation. Journal of Applied Physics. Vol. 12.

Brown P.T. and Booker J. R. 1985. Finite Element Analysis of Excavation. Computers and Geotechnics. Vol. 1, pp. 207-220.

Clough G. W., Sweeney B. P. and Finno, R. J. 1983. Measured Soil Response to EPB Shield Tunneling. Journal of Geotechnical Engineering, ASCE. 109(2): 131-149.

Dafalias Y. F. and Herrmann L. R. 1986. Bounding Surface Plasticity II: Application to Isotropic Cohesive Soils. Journal of Engineering Mechanics, ASCE. 112(12): 1263-1291.

Finno R. J. and Clough G. W. 1985. Evaluation of Soil Response to EPB Shield Tunneling. Journal of Geotechnical Engineering Division, ASCE. 111(2): 155-173.

Hawlader B.C., Lo K.Y. and Moore I. D. 2006. Analysis of tunnels in shaly rock considering three-dimensional stress effects on swelling. Canadian Geotechnical Journal. 42(1): 1-12.

Holt D. A. and Griffiths D. V. 1992. Transient Analysis of Excavations in Soil. Computers and Geomechanics. 13: 159-174.

Kasper T. and Meschke G. 2004. A 3D finite element simulation model for TBM tunnelling in soft ground. International Gournal for Numerical and Analytical Methods in Geomechanics. 28(14): 1441-1460.

Kaliakin V. N. 2005. Parameter estimation for time-dependent bounding surface models. Geo-Frontiers conference (2005); Soil constitutive models: evaluation, selection, and calibration. Geotechnical special publication. No. 128, pp. 237-256.

Kaliakin V. N. and Dafalias Y. F. 1990. Verification of the Elastoplastic-Viscoplastic Bounding Surface Model for Cohesive Soils. Soils and Foundations. 30(3): 25-36.

Kaliakin V. N. and Dafalias Y. F. 1991. Details Regarding the Elastoplastic-Viscoplastic Bounding Surface Model for Isotropic Cohesive Soils. Civil Engineering Report. No. 91-1, University of Delaware, Newark.

Kamemura K. and Kimura H. 1981. A Study for Tunnel Analysis Considering Face Progress. Gournal of Soil Mechanics and Foundation Engineering. pp. 1565-1568.

Lacerda W. A. 1976. Stress-Relaxation and Creep Effects on Soil Deformation. Ph.D. Thesis, University of California, Berkeley.

Lewis R. W. and Schrefler B. A. 1987. The Finite Element Method in the Deformation and Consolidation of Porous Media. John Wiley and Sons Ltd., London.

Pan X.D. and Hudson J.A. 1988. Simplified Three-Dimensional Hoek-Brown Yield Criterion. Proceedings of the International Society of Rock Mechanics (ISRM) Symposium. pp. 95-103.

Shalabi F.I. 2005. FE analysis of time-dependent behavior of tunneling in squeezing ground using two different creep models. Tunnelling and Underground Space Technology. 20(3): 271-279.

Swoboda G. and Abu-Krisha A. 1999. Three-Dimensional Numerical Modelling for TBM Tunnelling in Consolidated Clay. Tunnelling and Underground Space Technology. 14(2): 327-333.

Terzaghi K. 1943. Theoretical Soil Mechanics. John Wiley and Sons, Inc., NewYork.

Xiaoli Y., Linrong X., Liang L. and Baochen L. 2002. Effects of intermediate principal stress on the displacement around tunnels in visco-elastoplastic rock. Geotechnical Engineering. 33(2): 87-92.

Zienkiewicz O. C., Owen D. R. J. and Cormeau I. C. 1974. Analysis of Viscoplastic Effects in Pressure Vessels by the Finite Element Method. Nuclear Engineering and Design. Vol. 28. pp. 278-288.